JOURNAL OF APPLIED ELECTROCHEMISTRY 21 (1991) 32–39

Mass transfer at rotating cone electrodes

A. F. S. AFSHAR*, D. R. GABE

IPTME, Loughborough University of Technology, Loughborough LE11 3TU, UK

B. SEWELL

Twickenham Plating Group PLC, Colne Rd., Twickenham, Middlesex TW1 4JR, UK

Received 15 August 1989; revised 10 April 1990

Upright and inverted rotating cone electrodes (apex half angle 52°) have been studied using electrodeposition of copper from an acid electrolyte ($Sc = 1770$) by means of limiting current mass transport techniques. The behaviour suggests that it is appropriate to regard these electrodes as modified disc electrodes. The upright rotating cone electrode exhibits a flow transition at $Re = 1 \times 10^5$. In laminar flow $Sh = 4.5Re^{0.48}$ and in turbulent flow $Sh = 0.04Re^{0.95}$. The inverted rotating cone electrode exhibits a flow transition at $Re = 6 \times 10^4$. In laminar flow $Sh = 4.5Re^{0.45}$ and in turbulent flow $Sh = 0.04Re^{0.88}$. The data have been interpreted in terms of a coating thickness affected by throwing power effects and the use of a conical cathode cell for control of high speed electrodeposition processes is indicated.

Nomenclature

A	electrode area (cm^2)
C_b	concentration (of bulk solution) ($mol\,cm^{-3}$)
Δc	concentration difference ($mol\,cm^{-3}$)
D	diffusion coefficient ($cm^2\,s^{-1}$)
$f/2$	friction factor
F	Faraday's constant (96485 $A\,s\,mol^{-1}$)
i_L	limiting current density ($A\,cm^{-2}$)
J	mass transfer flux ($mol\,s^{-1}\,cm^{-2}$)
K_L	mass transfer coefficient ($cm\,s^{-1}$)
l	slant height of the cone (cm)
U	peripheral velocity ($cm\,s^{-1}$)
x	local condition coordinate (cm)
z	no. of electrons
α	apex half-angle of cone
ω	angular velocity ($rad\,s^{-1}$)
τ	wall shear stress ($dyn\,cm^{-2}$)
ν	kinematic viscosity ($cm^2\,s^{-1}$)
Re	Reynolds number $= Ud/\nu$
Sc	Schmidt number $= \nu/D$
Sh	Sherwood number $= K_L d/D$

1. Introduction

In recent years the rotating cone electrode has received some limited attention partly due to the simple model that can be invoked for both theoretical and experimental investigations of the boundary layer characteristics. However, most studies have related to heat transfer from which the comparability with electrochemical applications is generally thought to be direct: thus investigators such as Jordan *et al.* [1, 2] have exploited the heat to mass transfer analogy. On the other hand, investigators such as Subramaniyan *et al.* [3, 4] have extrapolated the classical Levich equations for a rotating disc electrode to use for a cone, the cone in extreme truncated form being a cylinder (apex angle of 0°) or a disc (apex angle of 180°). The nomenclature being employed is shown in Fig. 1, the apex half angle being α and l the slant height measured from the base of the cone.

The flow pattern of a rotating cone can be quite complex: at low rotational speed the flow is laminar all over the surface while at higher speeds laminar and turbulent flow can exist simultaneously. The laminar flow exists at the region where the radius of the electrode is small and the turbulent flow at the region where the radius is greater. However, due to changes in radius of the cone the flow can become very complex since the centrifugal force imparted to the adjacent liquid element depends on the distance from the apex of the cone, i.e. slant height or segment radius. Therefore, the liquid at a distance away from the apex will experience a greater centrifugal force and hence be expelled from the surface of the cone with a greater force than the liquid near the apex. This induces a tangential flow along the surface away from the apex which will affect the turbulent flow by reducing it for a given rotational speed.

Jordan *et al.* [1, 2] investigated the mass transfer to a stationary conical micro electrode and the flow round it. For laminar flow the mass transfer relationship took the form:

$$Sh = \frac{4}{3\sqrt{3}} Re^{0.5} Sc^{0.33} \quad (1)$$

In a comprehensive study of voltammetry at solids, they also constructed a conical platinum electrode

* Now at S. G. Owen Co. Ltd., Lodge Farm Industrial Estate, Northampton NN5 7UF, UK.

0021-891X/90 $03.00 + .12

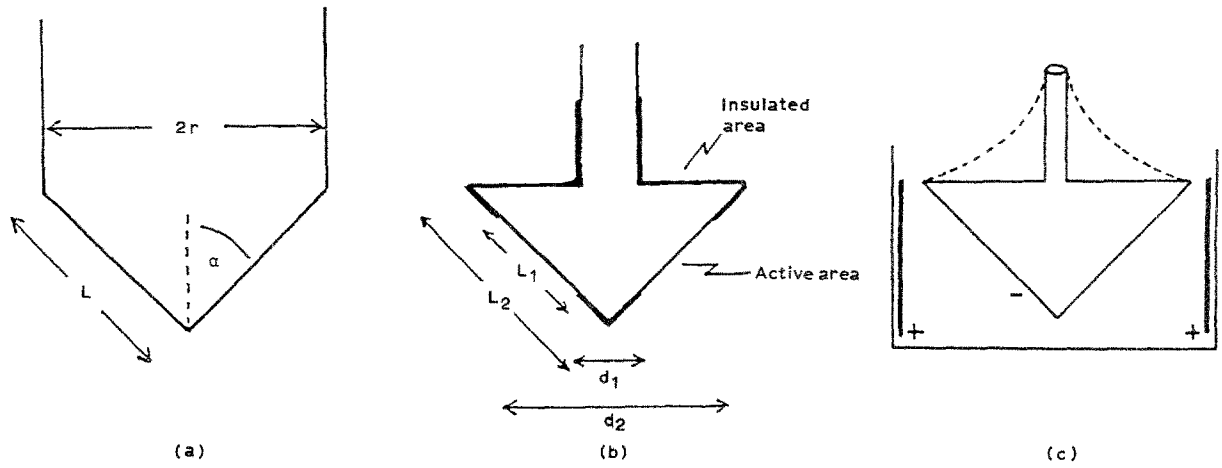

Fig. 1. Nomenclature and geometry for rotating cone and electrodes. (a) Inverted cone electrode, (b) ring cone electrode, and (c) schematic cell configuration.

with a slant height of 0.04 cm and a surface area of 0.003 cm^2. At 100% current efficiency, the mass transfer flux at the electrode surface was correlated with limiting current such that $i_L \propto C$ and $i_L \propto U^{0.5}$:

$$i_L = 0.77zFAC_b U^{0.5} D^{0.67} l^{-0.5} \nu^{-0.25} \quad (2)$$

where l denotes the slant height of the cone.

Tien [5] obtained a theoretical relationship for heat transfer in laminar flow at Prandtl number of 0.72, the mass transfer analogy being:

$$Sh = 0.329\left(\frac{l^2\omega \sin\alpha}{\nu}\right)^{0.5} \quad (3)$$

After considering his data he incorporated $Sc^{0.4}$ as follows:

$$\frac{Sh}{Sc^{0.4}} = 0.375\left(\frac{l^2\omega \sin\alpha}{\nu}\right)^{0.5} \quad (4a)$$

The agreement between this theoretical formula and the data obtained for different cones by Subramanyan *et al.* [3] was fairly good. Consequently, they plotted $Sh/Sc^{0.4}$ against $(l^2\omega \sin\alpha)/\nu$ and obtained an equation for cones with apex angle greater than 40° as

$$\frac{Sh}{Sc^{0.4}} = 0.345\left(\frac{l^2\omega \sin\alpha}{\nu}\right)^{0.5}. \quad (4b)$$

In contrast Kirowa-Eisner and Gileadi [6] adopted the equation for a rotating cone electrode derived by Newman and Mohr [7]; this gives the local mass transfer rate at the limiting current as

$$J = 0.62C_b(\nu\omega \sin\alpha)^{0.5} Sc^{-0.67} \quad (5)$$

and the overall mass transfer rate for a conical electrode of base radius r is

$$J_{total} = 0.62C_b r^2\left(\frac{\nu\omega}{\sin\alpha}\right)^{0.5} Sc^{-0.67}. \quad (6)$$

The above investigators treated the rotating cone as a modified rotating disc, hence the limiting current of the rotating cone is related to that of the rotating disc by

$$i_{L(cone)} = i_{L(disc)} (\sin\alpha)^{0.5}. \quad (7)$$

For conditions when the laminar–turbulent transition is approached Kappesser *et al.* [8] transformed the mass transfer equation in laminar flow for a disc given by Newman

$$\overline{Sh}_d = \frac{0.62048 Re_d^{0.5} Sc_d^{-0.67}}{1 + 0.2980 Sc_d^{-0.3} + 0.1451 Sc_d^{-0.67}} \quad (8)$$

to that of rotating cones by substituting the appropriate parameters and obtained the following expression

$$\overline{Sh}_c = \frac{0.62046 Re_c^{0.5} Sc_c^{-0.67}}{1 + 0.2980 Sc_c^{-0.33} + 0.1451 Sc_c^{-0.67}} \quad (9)$$

where $\overline{Sh}_c = \bar{J}l/D\Delta C$, and $Re_c = \omega r l/\nu = (\omega l^2 \sin\alpha)/\nu$ and where subscripts d and c denote disc and cone, respectively.

The above equation was valid for experimental results in the range

$$0.7 < (Sc, Pr) < 2.4.$$

For turbulent flow, Kreith [9] used the Reynolds analogy to obtain an expression for the heat transfer for a rotating cone at a Pr number of unity, according to Kappesser. The results are in good agreement with the experimental data for $0.7 < (Pr, Sc) < 2.4$. However Kreith extended his work in order to determine the heat and mass transfer for Prandtl or Schmidt numbers differing from unity. The final result is

$$Sh_x = 0.0212(2.6)^{0.2} Re_x^{0.8} \times \left(\frac{Sc}{1 + (f_x/2)^{0.5} 5Sc + 5\ln(5Sc + 1) - 14}\right) \quad (10)$$

where x denotes local condition, $(f_x/2)$ is the local friction factor given by $\tau/\rho\omega x^2(\sin\alpha)^2$ and τ is the wall shear stress in Pa.

Alternatively, Kappesser [8] proposed a simplified expression

$$Sh_x = 0.0182 Re_x^{0.9} Sc^{0.25} \quad (11)$$

and to account for the effect of laminar flow over the surface of the cone near the apex, the following

expression was given by the investigator

$$\overline{Sh} = [\overline{Sh}_L - \overline{Sh}_T]\frac{x_c}{l} + \overline{Sh}_T \qquad (12)$$

where x_c is the distance to flow transition, which can be obtained from the results of Kreith *et al.* [9], $\overline{Sh}_L$ is the laminar Sherwood number, and $\overline{Sh}_T$ is the turbulent Sherwood number.

Experimental results obtained by Kappesser *et al.* [8] indicate a good agreement between theory and experiment. Previous applications for the rotating cone electrode include heat transfer probes and voltammetric analysis but in this investigation it was also exploited in a current density or throwing power cell, akin to the Hull cell, where the rotation rate provided solution agitation to a well-quantified degree.

2. Experimental details

The geometry of the cone electrodes was based on two design requirements. Firstly, that the electrodes would be used in existing rotating electrode rigs employed normally with cylinder and disc electrodes in applications related to electrodeposition where currents of up to 10 A are normally used. Secondly, that the geometry should be determined by the need to simulate the Hull cell current distribution pattern, a concept discussed fully elsewhere [10]. Consequently, the small size of Jordan's voltammetric microelectrode [1, 2] was considered inappropriate and the cone apex angle was not one used hitherto although is within the ranges used previously. The circular cones had the parameters given in Table 1.

The cones were machined from solid stainless steel and partially hollowed to reduce weight and rotational inertia. The basal disc was stopped off at all times to maintain electrodeposition on the curved surface only. Using copper as a model cathodic deposit nitric acid (50%) could be employed to dissolve the coating while the stainless steel was fully passivated and effectively inert – thus after many months of continual usage the dimensions of the stainless steel cones remained unaltered.

Acid copper sulphate solution was used as a model electrolyte at three concentrations but especially 0.014 M and 0.07 M with 0.5 M sulphuric acid as support electrolyte. The mass transport characteristics of these solutions were well-established from previous investigations [11, 12]. Specifically, those were: $\nu = 1.0184 \times 10^{-2}\,cm^2\,s^{-1}$, $D = 5.84 \times 10^{-6}\,cm^2\,s^{-1}$, and $Sc = 1770$.

The rotating electrode rigs have been described in earlier papers [11, 12] and could be operated at up to 1000 rpm ($Re = 5 \times 10^5$) in a good reproducible manner. Current was supplied by a Thompson 'Ministat' at up to 15 A under potentiostatic control, using a saturated mercury/mercurous sulphate (MMS) reference electrode (RE), via a silver-graphite brush system. Rotation rates were measured by a tachometer which was calibrated using a stroboscope. The motor incorporated tachometer feedback and was very stable in operation; using a three-point bearing and careful alignment of the rotor shaft eccentric rotation could be eliminated despite the heavy cone electrodes.

Table 1. Dimensions of experimental cones.

Parameters	*Inverted cone*	*Upright cone*
Basal diameter (mm)	194	128
Slant height (mm)	77.5	69
Apex half angle	52°	52°

Mass transfer was measured by the limiting current method using both the traditional potentiodynamic (sweep) techniques at 1–10 mv s^{-1} and the potential-step method, in which a potential corresponding to the limiting current plateau is determined in preliminary experiments and then applied as a potentiostatic condition. This latter technique has been shown to be reliable in conditions of substantial agitation [13, 14]. Because the main application for a conical electrode cell is in simulation of coating thickness variations due to throwing power (or secondary current distribution) effects the same presentation approach was used as for Hull cell data. This approach converts the coating thickness variation to an equivalent deposition current density at 100% cathodic efficiency and can be achieved either by direct coating thickness measurement or by measuring the overpotential profile on the electrode surface and converting it to an equivalent current density by means of the polarization curve obtained under those conditions of rotation. Thus, in this study, coating thicknesses were established by X-ray fluorescence analysis using a Fischerscope XM1500 and the current profile obtained by placing a Luggin reference electrode probe at various positions on the slant height surface during potentiodynamic sweeping. In these manners an equivalent current density profile was determined at each rotation rate, typically 0, 20, 50, 80, 120, 160, 200, 250, 300, 350, 400 etc. r.p.m.. Agreement between the two methods was in general good, discrepancies being attributable to either rough deposits developing early or low current efficiencies.

3. Results

All the mass transfer data presented here was obtained with the same electrolyte and at the same temperature so is directly comparable in that respect. For the inverted rotating cone electrode, limiting current densities were obtained for the whole cone using the reference electrode placed at different positions on the sloping surface. Figure 2 shows data for the RE at a slant height of 31 mm and exhibits three distinct regions. The first region of laminar flow has a slope of about 0.49 and the last region of turbulence a slope of about 1.0; the intermediate transition region has a gradually increasing slope as the increasing rotation rate results in an increasing limiting current. If other positions on the sloping surface are used for RE control a broadly similar pattern was found (Fig. 3) and

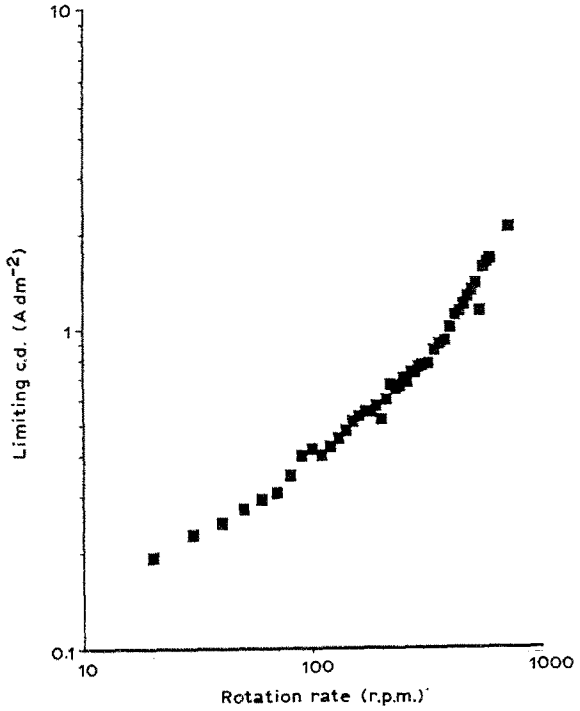

Fig. 2. Limiting current density values on the inverted rotating cone electrode at slant height of 31 mm for 0.014 M Cu^{2+}.

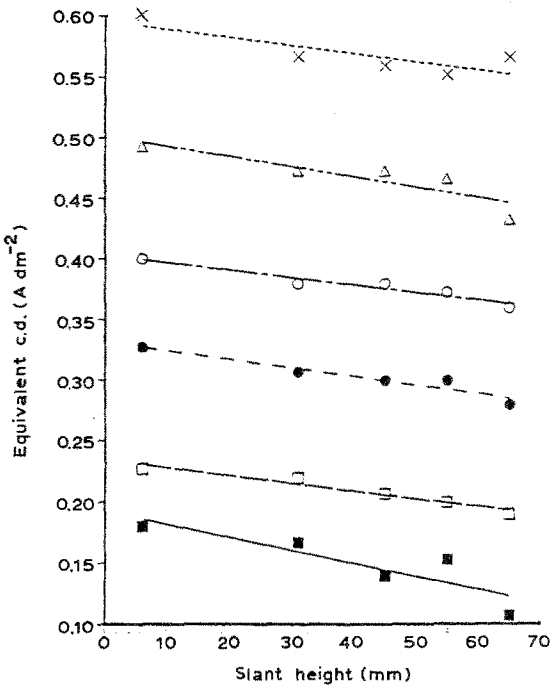

Fig. 4. Equivalent current density distribution on the inverted rotating cone electrode at six low rotation rates for 0.014 M Cu^{2+}. Rate: (■) 0, (□) 20, (●) 50, (○) 80, (△) 120, and (×) 160 r.p.m.

taking an average of such data the two flow region slopes were slightly lower in value (0.46 and 0.79, respectively). Figures 4 and 5 show the coating thickness variation over the inverted cone surface, due to throwing power, expressed as an equivalent current density for a series of rotation rates. Figure 4 relates primarily to behaviour in the laminar flow regime and Fig. 5 in transition and turbulent flow (i.e. > 160 r.p.m.). The slopes show a reasonable consistency and are typical of a larger mass of data obtained at that stage.

A similar investigation was carried out for the vertical rotating cone electrode and using a RE control position at 38 mm slant height total current density values were determined (Fig. 6). The form is essentially similar to the inverted cone (Fig. 2) but the laminar and turbulent region slopes are approx. 0.39 and 1.05, respectively. By again taking a series of RE control positions a family of curves can be obtained and the reproducibility was very good (Fig. 7). The throwing power effect observed as deposit thickness variation was again studied at many rotation rates and the laminar and turbulent flow data shown separately as equivalent current density values as before (Figs 8

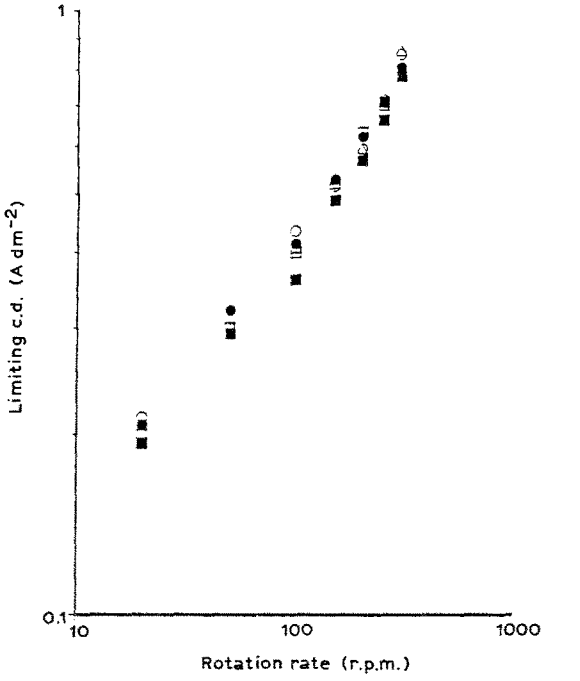

Fig. 3. Limiting current/rotating rate relationship on the inverted rotating cone electrode at five slant heights for 0.014 M Cu^{2+}. Slant heights: (■) 75, (□) 58, (●) 38, (○) 22, and (△) 5 mm.

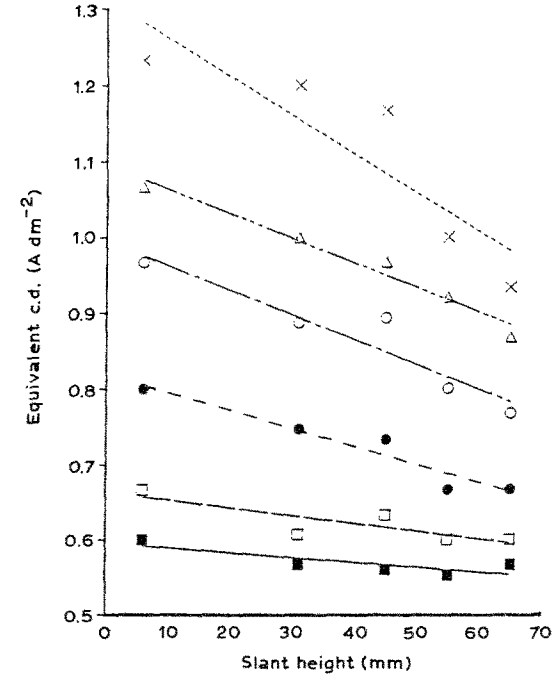

Fig. 5. Equivalent current density distribution on the inverted rotating cone electrode for six higher rotation rates for 0.014 M Cu^{2+}. Rate: (■) 160, (□) 200, (●) 250, (○) 300, (△) 350, and (×) 400 r.p.m.

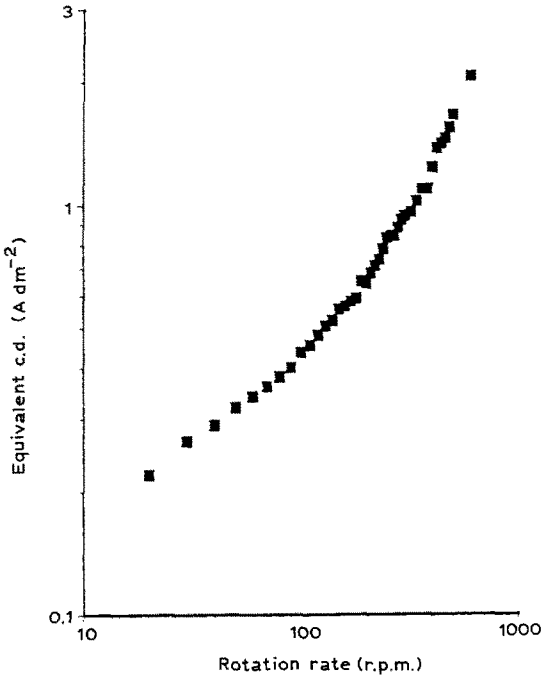

Fig. 6. Limiting current/rotation rate relationship on the upright rotating cone electrode at slant height of 38 mm for 0.014 M Cu^{2+}.

and 9). Clearly the transition occurs in a similar manner and rotation rate on both conical electrodes.

One of the purposes of this study was to examine and possibly exploit the current density distribution patterns through the consequent deposit thickness profiles: this is described elsewhere [10]. The mass transfer analysis can be related to deposit structure, however, and scanning electron microscopy was employed to characterize the surface morphology. In the case of copper from this type of electrolyte deposition at the limiting current density is characterized by a nodular growth mode developing into loose powdery deposits. Throughout this study normal characteristics were observed but a changing nodule density along the conical surface was generally observed. In Fig. 10 scanning electron micrographs illustrate this observation at slant height positions of 7, 42 and 64 mm on the inverted rotating cone electrode. While these structure refer to differing deposit thicknesses the fundamental relationship is with the equivalent current densities prevailing at those positions.

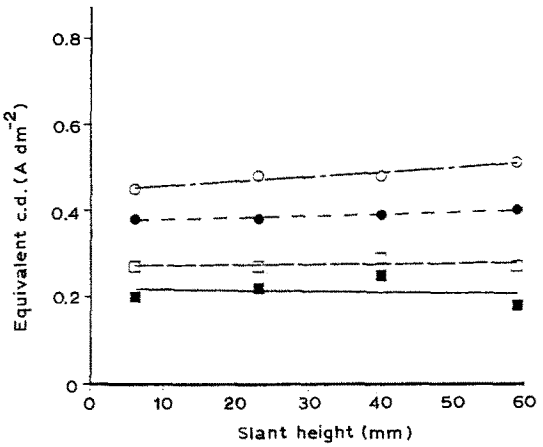

Fig. 8. Limiting current density distribution on the upright rotating cone electrode at four lower rotation rates for 0.014 M Cu^{2+}. Rates: (■) 0, (□) 20, (●) 50, and (○) 80 r.p.m.

4. Discussion

It has already been pointed out that this study was not predominantly mass-transfer oriented and therefore no attempt has been made to provide a rigorous mass transfer correlation. In particular, no attempt has been made to systematically vary the physical properties of the electrolyte such as viscosity and ion diffusion coefficient and so a dependence upon the Schmidt number ($Sc = \nu/D$) cannot be derived from

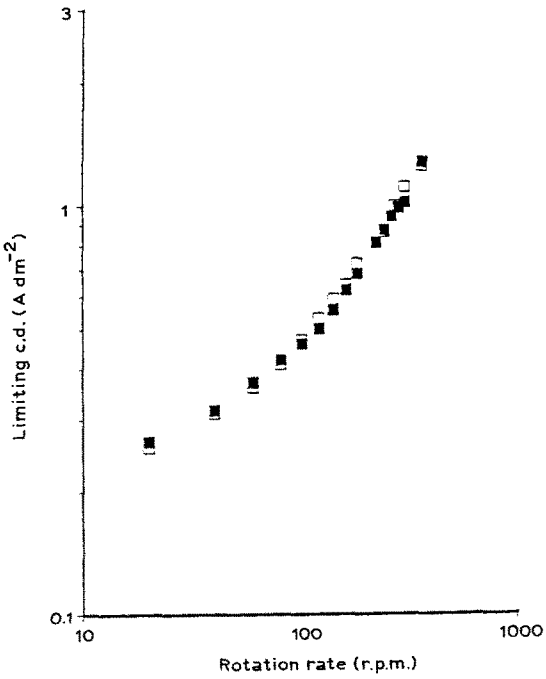

Fig. 7. Limiting current/rotation rate relationship on the upright rotating cone electrode for 0.014 M Cu^{2+}. Slant heights; (■) 17 mm and (□) 57 mm.

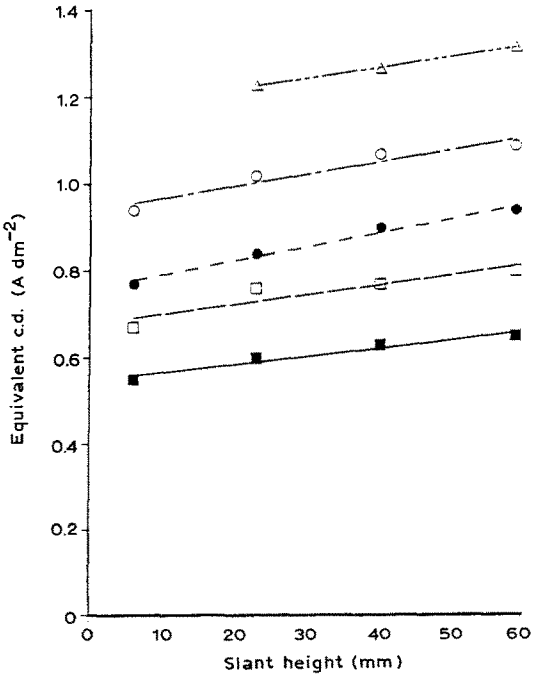

Fig. 9. Limiting current density distribution on the upright rotating cone electrode at five higher rotation rates for 0.014 M Cu^{2+}. Rates: (■) 120, (□) 160, (●) 200, (○) 250, and (△) 300 r.p.m.

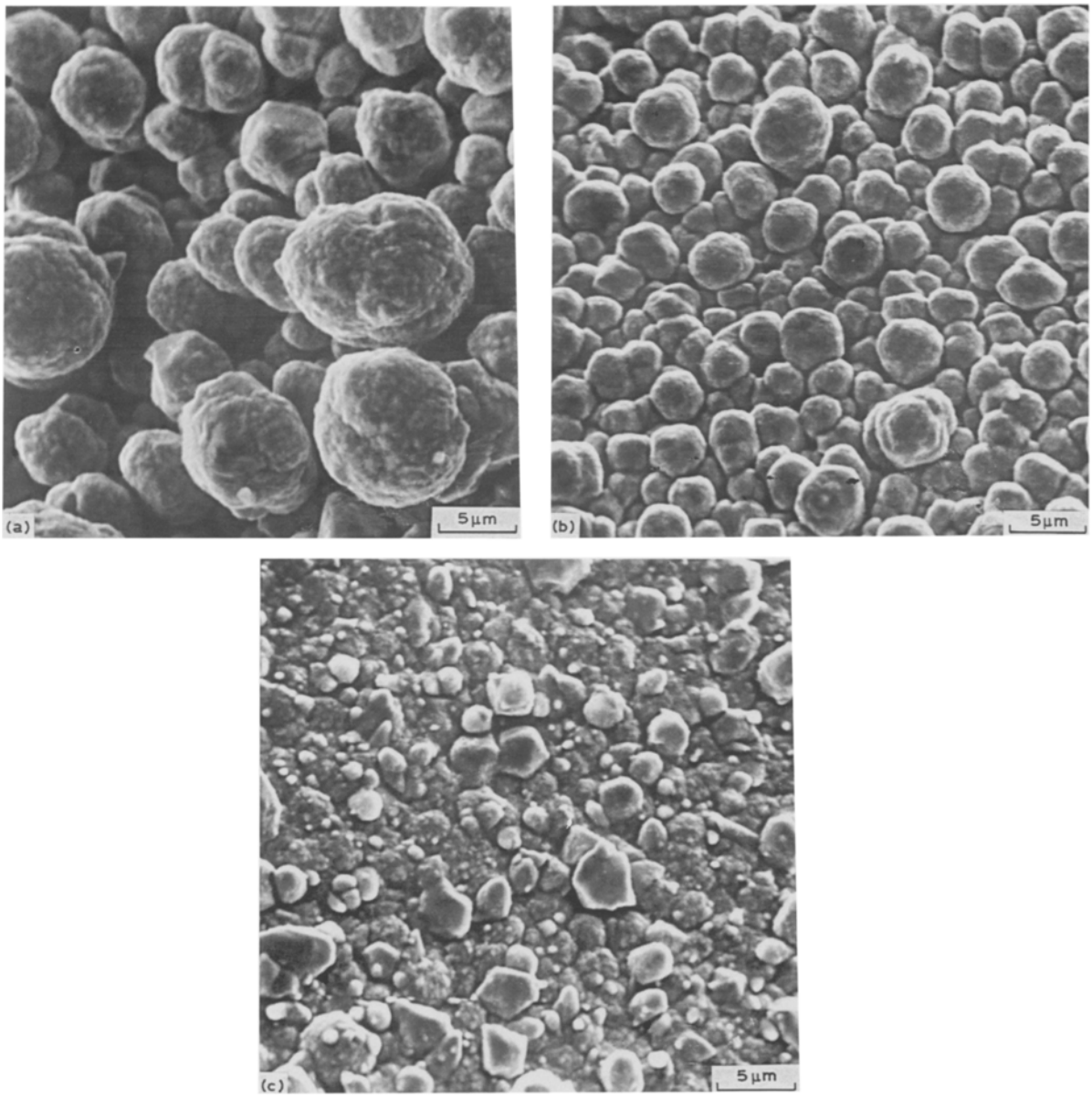

Fig. 10. SEM micrographs of the inverted rotating cone electrode surface during deposition of copper at slant heights of (a) 7, (b) 42, and (c) 64 mm. Magnification 5000×.

this work. However, the dependence of mass transfer upon rotation rate and the Reynolds number ($Re = U_d/\nu$) was of importance and was considered at length.

As has been shown by the experimental results two flow regions, together with a transition, can be seen in the data presented graphically. The data have been analysed on the basis of the relationships

$$i_L = k_1 U^a \quad \text{or} \quad Sh = k_2 Re^n$$

where k_1 and k_2 are cleraly different but the index n is characteristic of the laminar and turbulent regions. Values of n obtained have been averaged as follows

Upright cone	laminar	$n = 0.48 \pm 0.1$
	turbulent	$n = 0.93 \pm 0.12$
Inverted cone	laminar	$n = 0.45 \pm 0.04$
	turbulent	$n = 0.88 \pm 0.22$

Using the nomenclature discussed earlier this gives mass transfer relationships as following.

For the upright cone:

$$\text{laminar region} \quad Sh = 4.5Re^{0.48}$$

$$\text{or} \quad i_L = 4.5zFCD\omega^{0.48} l^{1.48} \nu^{0.48} (\sin\alpha)^{0.48}$$

$$\text{turbulent region} \quad Sh = 0.04Re^{0.93}$$

$$\text{or} \quad i_L = 0.04zFCD\omega^{0.93} l^{1.93} \nu^{-0.07} (\sin\alpha)^{0.93}$$

For the inverted cone:

$$\text{laminar region} \quad Sh = 4.0Re^{0.45}$$

$$\text{or} \quad i_L = 4zFCD\omega^{0.45} l^{1.45} \nu^{-0.55} (\sin\alpha)^{0.45}$$

$$\text{turbulent region} \quad Sh = 0.04Re^{0.88}$$

$$\text{or} \quad i_L = 0.04zFCD\omega^{0.88} l^{1.88} \nu^{-0.12} (\sin\alpha)^{0.88}$$

In recent years several papers have been published concerning mass transfer at cones but data have been shown graphically in different forms and in the absence of published numerical values transformation is difficult. However, data can be compared by replotting results obtained here. For example, Subramaniyan

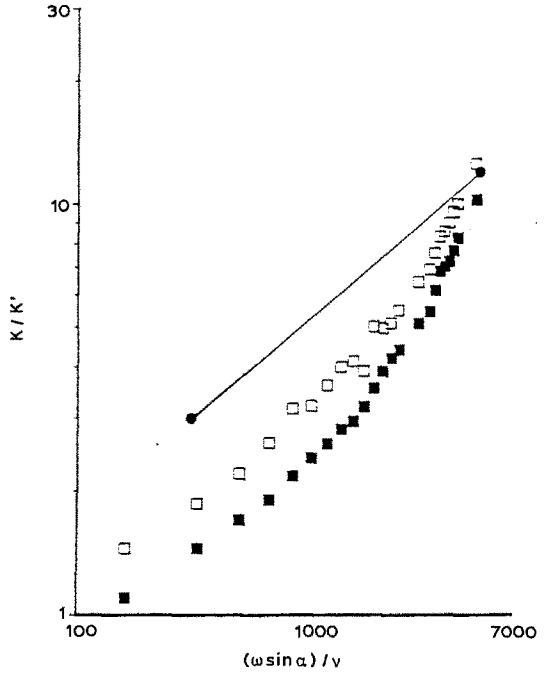

Fig. 11. Mass transfer relationship for the upright and inverted rotating cone electrodes using format of Subramaniyan *et al.*

et al. [3, 4] plotted their mass transfer results in two ways: $\log(Sh/Sc^{0.4})$ against $\log(Re)$ and $\log(K_L/K'_L)$ against $\log(\omega \sin\alpha)/\nu$. The second approach has been used in Fig. 11 and the agreement on the gradient, and thus the indice in the laminar region, is excellent (Subramaniyan *et al.* do not have data for the turbulent region). The ratio K_L/K'_L is in effect an enhancement ratio comparing limiting currents obtained during rotational and during stationary periods for the cone; it has been found to be not entirely reliable because natural convection at surfaces of differing surface condition shows considerable variability and therefore a low rotation rate of 50 r.p.m. has been preferred to the stationary condition as a base point. This explains why the enhancement factors in the present work appear to be depressed.

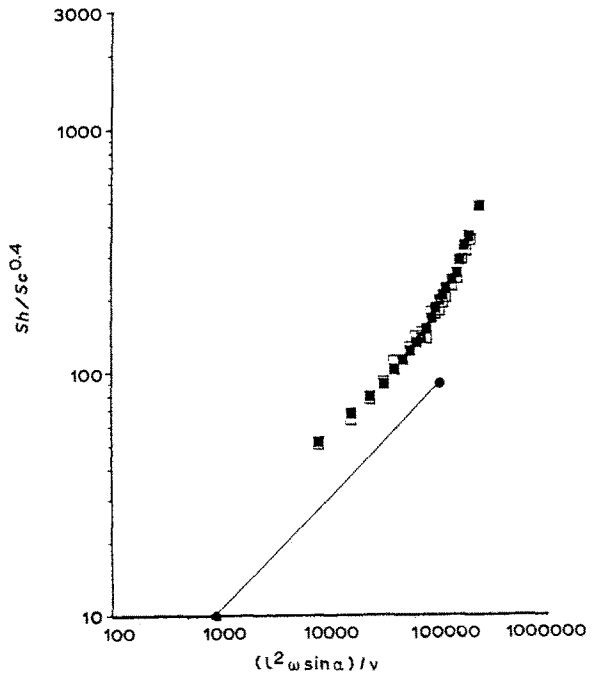

Fig. 12. Mass transfer relationship for the upright and inverted rotating cone electrodes using format of Subramaniyan *et al.*

Subramaniyan *et al.* used an alternative graphical representation and data have been compared on this basis in Fig. 12 again only for the laminar region. Agreement is again reasonable the presumption being that the cone is a truncated disc with the approximation being good if the apex angle $\alpha > 40°$ which it is. Thus the general relationship is $Sh/Sc^{0.4} = 0.345Re^{0.5}$ where $Re(\text{disc}) = d^2\omega/\nu$ and $Re(\text{cone}) = (l^2\omega \sin\alpha)/\nu$. Thus for cones $K_L/K'_L = 0.169\ (\omega \sin\alpha)/\nu)^{0.5}$. On that basis, the present data gives the following relationships

$$\text{laminar region} \quad Sh/Sc^{0.4} = 0.9Re^{0.5}$$

$$\text{turbulent region} \quad Sh/Sc^{0.4} = 0.001Re^{0.9}$$

The numerical disagreement may be attributed to the fact that Schmidt numbers were different (Subramaniyan $Sc = 1100$, this study $Sc = 1770$) and were not varied systematically in either case. Because the Schmidt number was not varied it is not possible to give a critical assessment of the expression given by Kappesser *et al.* (see Equations 8 and 9) except to indicate that the data obtained is consistent with such an expression.

The laminar/turbulent transition in the present studies can be seen to occur at $Re \approx 10^5$, in fact it is $Re = 1 \times 10^5$ for the upright rotating cone and $Re = 6 \times 10^4$ for the inverted rotating cone. This is similar to values reported previously, both Kreith [9] and Kappesser *et al.* [8] indicating that it varies with the apex angle of the cone being typically $Re = 1.5 \times 10^5$ at $\alpha = 60°$ and $Re = 2.5 \times 10^5$ when $\alpha > 90°$. In particular Kappesser *et al.* [8] correlated data for cones of apex angle 30°, 60°, 90°, 120° and 180° in solutions of high Schmidt number using relationships as in Equations 8 and 10. This approach is used in Fig. 13 which indicates that the difference in mass transfer between upright and inverted cones is really very small (the apex angle was of course identical) and that the transition was essentially similar. The further implications of the approach of Kappesser *et al.* cannot be confirmed here, because a cone of constant apex angle was employed throughout, but are worth mentioning. They are that in the laminar region the gradient of the Sh/Re graph should be independent of cone apex angle whereas in the turbulent region the

Table II. Comparison of rotating electrodes

$Sh = const\ Re^n$			
Rotating Electrode System	*n Laminar*	*n Turbulent*	*Transitional* Re_{crit}
Disc (RDE)	0.5	0.9	10^5
Cylinder (RCE)	0.33	0.67	2×10^2
Hemi-sphere	0.5	0.67	2×10^4
Inverted cone	0.45	0.88	6×10^4
Upright cone	0.48	0.93	1×10^5
Annular flow	0.33	0.58	2×10^3

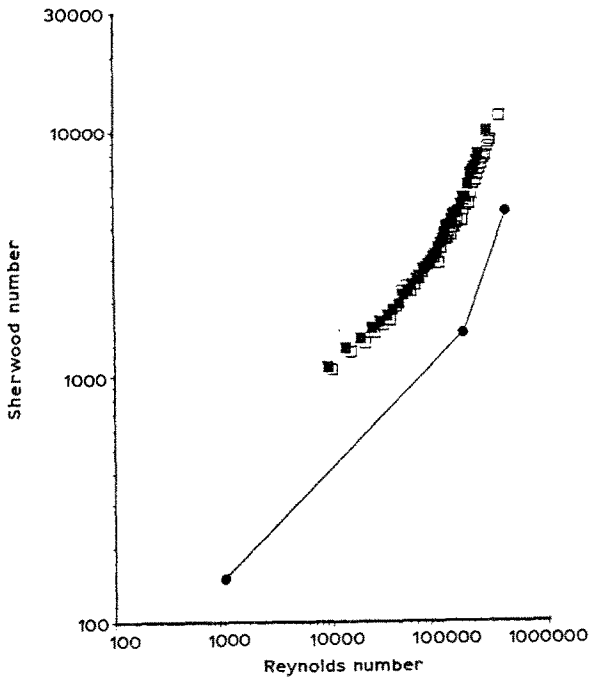

Fig. 13. Mass transfer relationship for upright and inverted rotating cone electrodes using format of Kappesser *et al.*

slope should increase with increasing apex angle. And further that any increase in the apex angle should extend the laminar region by delaying the transition to higher values of *Re*: judging by the experimental evidence this effect is quite small. It is, however, worth reiterating that the rotating conical electrode is in every respect much more like the disc electrode rather than the cylinder electrode, thus justifying the approach of Kirowa-Eisner and Gileadi [6] (see Equation 7) who regarded the cone as a truncated disc. It may be useful in some contexts to regard the cone as an intermediate geometry when broad mass transfer behaviour is compared in a simplistic manner, typical numerical comparison being given in Table 2.

The consequence of this geometrical analogy is that two types of fluid mixing are observed with the rotating cone. Firstly, the rising laminar flow characteristic of the rotating disc geometry. For the upright cone this is limited largely to the basal disc which in this study was always insulated and so took no part in the mass transport reactions. In the inverted cone it gave rise to an upward centrifugal pumping action which was clearly seen and tended to magnify 'edge' effects at the apex where the deposit thickness was always greatest. Secondly, vortex mixing with the vortices increasing in size with an increase in the rotation rate and decreasing as the slant height decreases. The consequence is that for the upright cone the pumping action is downwards – the reverse of the inverted cone – creating a whirlpool effect. With these marked differences in flow pattern it is therefore somewhat surprising that the overall mass transport behaviour is so similar: the mass transfer data shows in fact that two cone configurations are quite similar in behaviour but that the difference can be quantitatively defined.

The application of this type of cone electrode is primarily seen as a throwing power cell; this is discussed in detail elsewhere [10]. However, it needs to be stated that the Hull cell geometry influenced the decision to use cones having apex half angles of 52° in order to maintain geometric similarity. In the Hull cell deposit thickness variation over the cathode panel is expressed as an equivalent current density and the relationship is logarithmic. No agitation is employed. The importance of Figs 4, 5, 8 and 9 can now be appreciated because the Hull cell relationship has been found with the added dimension of rotation rate which is in effect an agitation parameter. By use of this agitation parameter a dynamic or agitated Hull cell is now feasible in order to simulate highly agitated industrial processes in the laboratory or to provide a basis for similarity studies between processes using differing modes of agitation.

References

[1] J. Jordan, C. A. Javick and W. E. Ranz, *Anal. Chem.* **27** (1955) 1708.
[2] J. Jordan, C. A. Javick and W. E. Ranz, *J. Am. Chem. Soc.* **80** (1958) 3846.
[3] V. Subramaniyan, M. S. Krishna and P. Adwarahan, *Indian J. Technol.* **4** (1966) 353.
[4] V. Subramaniyan, M. S. Krishna and P. Adwarahan, *Chem. Age India* **18** (1967) 202.
[5] C. Tien, *J. Heat Transf.* **8** (1965) 411.
[6] E. Kirowa-Eisner and E. Gileadi, *J. Electrochem. Soc.* **123** (1976) 22.
[7] C. M. Mohr and J. Newman, *J. Electrochem. Soc.* **123** (1976) 1687.
[8] R. Kappesser, R. Greif and I. Cornet *Appl. Sci. Res.* **28** (1973) 442.
[9] F. Kreith, *Appl. Sci. Res.* **11** (1962) 430.
[10] A. F. S. Afshar, D. R. Gabe and B. Sewell, *Trans. IMF* (to be published).
[11] D. R. Gabe and F. C. Walsh, *J. Appl. Electrochem.* **14** (1984) 555, 565.
[12] D. R. Gabe and P. A. Makanjuola, *J. Appl. Electrochem.* **17** (1987) 379.
[13] D. R. Gabe and P. A. Makanjuola, *Inst. Chem. E. Symp. Ser.* **98** (1986) 309.
[14] Mehrdad R. Kalantary and D. R. Gabe, *Trans. IMF* **67** (1989) 24, 28.
[15] A. M. Ahmed and G. H. Sedahmed, *J. Appl. Electrochem.* **18** (1988) 196.
[16] J. A. Paterson, R. Greif and I. Cornet, *Int. J. Heat Mass Transf.* **16** (1973) 1017.
[17] R. N. Smith and R. Greif, *Int. J. Heat Mass Transf.* **18** (1975) 1249.
[18] Ching-Sheng Wu, *Appl. Sci. Res.* **A8** (1959) 140.
[19] M. G. Fouad and A. M. Ahmed, *Electrochim Acta* **14** (1969) 651.
[20] U. Bohm, *Electrochim. Acta* **15** (1970) 1841.
[21] J. R. Lloyd, E. M. Sparrow and E. R. G. Eckert, *Int. J. Heat Mass Transf.* **15** (1972) 457.
[22] M. A. Partick, A. A. Wragg and D. M. Pargeter, *Can. J. Chem. Eng.* **55** (1977) 432.
[23] C. L. Tien and D. T. Campbell, *J. Fluid Mech.* **17** (1963) 105.
[24] C. L. Tien, *Int. J. Heat Mass Transf.* **8** (1965) 411.